DIVERSE O ISOTOPIC COMPOSITIONS OF VAPOR-PHASE CONDENSATES IN A LIKELY-COMETARY IDP. K. L. Utt[1], R. C. Ogliore[1], N. Liu[1], D. E. Brownlee[2], and D. J. Joswiak[2]. [1]Department of Physics, Washington University in St. Louis, St. Louis, MO 63130, USA [2]Department of Astronomy, University of Washington, Seattle, WA 98195, USA

Introduction: Filamentary crystals were first predicted to form via vapor-to-solid condensation of nebular gas and be accreted into comets [1]. Roughly 20 years later, filamentary crystals (i.e., whiskers, ribbons, or platelets) of low-Fe clinoenstatite were found in CP-IDPs [2]. In line with its predicted growth mechanism, filamentary enstatite in IDPs contains crystallographic defects indicative of direct condensation from vapor.

Filamentary enstatite crystals are commonly found in anhydrous IDPs but appear to be very rare in chondritic meteorites — there have been reports of individual elongated enstatite crystals in Paris (CM) [3], QUE 99177 (CR2) [4], and Bishunpur (LL3.1) [5]. This disparity of abundance is not solely explained by survivorship bias: filamentary crystals are substantially more tolerant of mechanical stress than their equiaxial counterparts [6] and are likely to have survived incorporation into asteroid parent bodies [1]. Fine-grained crystalline pyroxenes similar in size to typical filamentary enstatite crystals are regularly found among primitive chondrite matrix material [7, 8], suggesting that the survival of filamentary enstatite in meteoritic samples is possible. The relationship between cometary and meteoritic filamentary enstatite, if any, remains unclear.

The vapor-phase growth mechanism of cometary filamentary enstatite means that it reflects the isotopic composition of the gas from which it formed — crystals that condensed from a gas of solar isotopic composition would have O isotopic compositions similar to the ^{16}O-rich solar composition [9], while crystals that condensed from vaporized dust in the protoplanetary disk would have O isotopic compositions similar to that of the vaporized solids. Here, we report O isotopic measurements of four filamentary crystals from U2-20 GCP, a giant cluster IDP of likely cometary origin [10, 11].

Methods: We identified two whiskers (Samples A and B) and two ribbons (Samples C and D) in U2-20 GCP, shown in Fig. 1. Using a computer-controlled Omniprobe micro-manipulator in an FEI Quanta 3D FIB, we transferred the samples from a TEM grid to a sputter-cleaned Au foil mount. Grains with similar sizes from crushed Norton County (low-Ca aubrite) were placed within $10\,\mu\mathrm{m}$ of each sample as an isotope reference. This sample preparation allowed for the simultaneous measurement of the sample and the standard in a single scanning ion raster image.

We acquired $12 \times 12\,\mu\mathrm{m}$, $256 \times 256\,\mathrm{pixel}$ ion raster images using the Wash U Cameca NanoSIMS 50. Each sample was pre-sputtered with a $78\,\mathrm{pA}$ Cs^+ beam

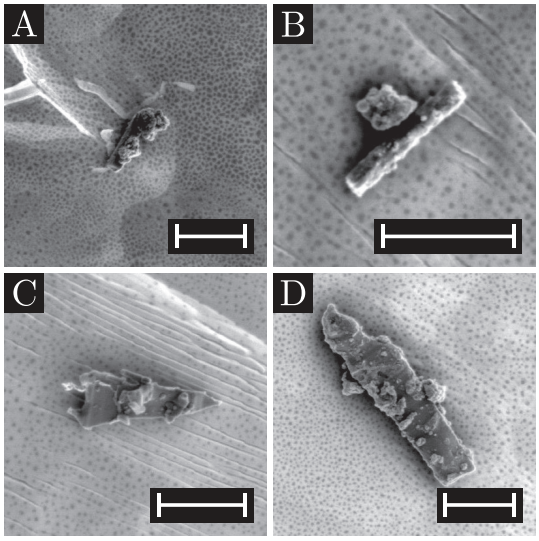

Figure 1: SE images ($2\,\mathrm{kV}$) of studied samples from U2-20 GCP. (a–b) Probable enstatite whiskers; (c–d) probable enstatite ribbons. Scale bars = $2\,\mu\mathrm{m}$.

for $\sim 300\,\mathrm{s}$ to remove any adsorbed water. Measurements were collected using a $2\,\mathrm{pA}$ Cs^+ primary beam focused to $\sim 100\,\mathrm{nm}$. We collected $^{16}O^-$, $^{17}O^-$, and $^{18}O^-$ simultaneously on separate electron multipliers. For all four samples, the mass-resolving power for $^{17}O^-$ was $\sim$5500, sufficient to resolve the interference from $^{16}OH^-$. We collected 100 frames (2.5 hours) for each sample, after which the enstatite whiskers (Samples A and B; see Fig. 1) were entirely consumed. Material from the enstatite ribbons (Samples C and D; see Fig. 1), however, remained after the measurements.

Data were analyzed with the L'image NanoSIMS analysis software (developed by L. Nittler) using regions of interest that were defined to avoid grain edges and minimize topography-induced instrumental mass fractionation effects. To minimize low count-rate sampling errors, pixels with $<7500\,\mathrm{cts}$ were excluded. Isotope images were aligned and corrected for electron multiplier deadtime ($42\,\mathrm{ns}$). Reported errors are dominated by the large statistical uncertainties associated with volumetrically-small samples.

Results: Of the four studied samples, three (Samples A, C, and D) have O isotopic compositions similar to ^{16}O-rich refractory inclusions in chondrites (CAIs and AOAs) [12, 13]. Sample C was found to be extremely ^{16}O-rich, with $\Delta^{17}\mathrm{O} = -23 \pm 21‰$ (2σ) — similar in composition to the Sun [9] and exceedingly rare CAIs with solar O isotopic compositions [14–16]

(see Fig. 3). Sample B was found to have an unusual isotopic composition with $\Delta^{17}O = 53 \pm 111‰$ (2σ). However, large statistical uncertainties due to the sample's small size prevent us from drawing strong conclusions about this point.

Table 1: Results for each sample (see Fig. 1) with 2σ confidence intervals.

	$\delta^{18}O$	$\delta^{17}O$	$\Delta^{17}O$
A	-36 ± 17	-33 ± 40	-15 ± 41
B	-63 ± 46	20 ± 109	53 ± 111
C	-85 ± 9	-67 ± 21	-23 ± 21
D	-38 ± 6	-43 ± 14	-24 ± 14

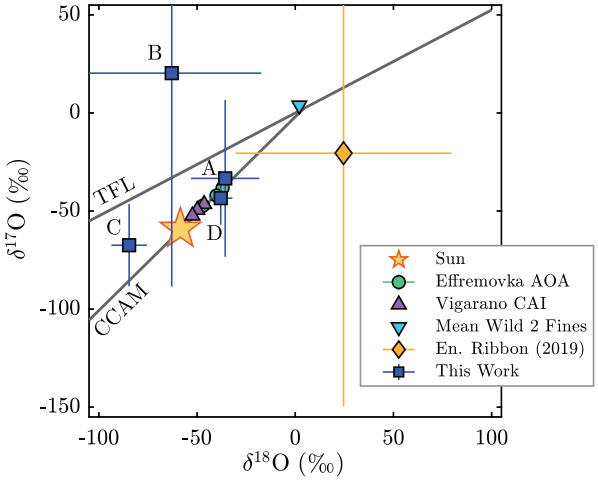

Figure 2: Oxygen three-isotope plot of studied samples (2σ uncertainties) compared to the Sun [9], Efremovka AOA [12], Vigarano CAI [12], comet Wild 2 fines [17], and a previously studied ribbon from U2-20 GCP [11].

Conclusions: We measured the O isotopic composition of four probable filamentary enstatite crystals from giant cluster IDP U2-20 GCP. Incorporating data from a previously measured enstatite ribbon from the same particle [11], we found wide variability in isotopic composition between five different filamentary particles (two whiskers and three ribbons) from the same giant-cluster IDP (derived from a single parent body). One ribbon (Sample C) is consistent with condensing directly from a gas of solar O isotopic composition, and another (Sample D) may have condensed in the same gaseous reservoir from which AOAs in chondrites formed [22]. The previously studied ribbon [11], however, is inconsistent with ^{16}O-rich refractory inclusions at the 2σ level. Our results suggest two possible formation scenarios: (1) the ribbon is an inner solar system condensate that was transferred to the outer solar system by preferential coupling to the gas [23], or (2) the ribbon formed by condensing from a ^{16}O-rich gas reservoir in the outer solar system. Future work includes TEM investigation of the two remaining ribbons (Samples C and D) to determine their crystal structures. Combining isotopic data with detailed crystallography will help to distinguish or constrain the potential formation scenarios for these samples.

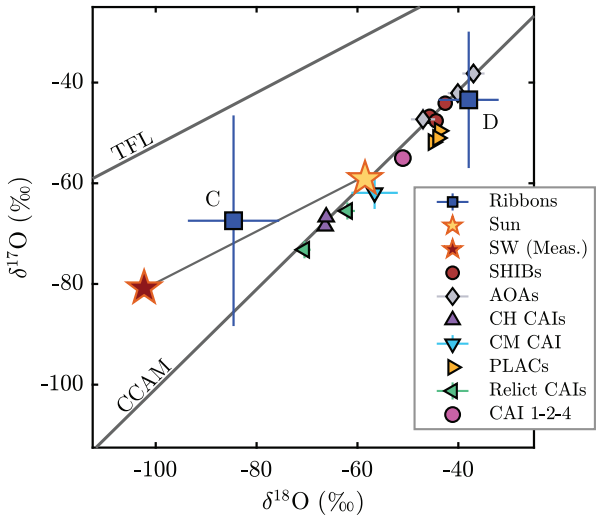

Figure 3: Samples C and D compared to other ^{16}O-rich solar system objects: the Sun and Genesis measurements [9], spinel-hibonite inclusions (SHIBS) [18], Efremovka AOA [12], CH CAIs [19], CM CAI [20], platy crystal fragments (PLACs) [21], relict CAIs [15], and CAI 1-2-4 [14]. Uncertainties are 2σ.

References: **[1]** B. Donn and G. W. Sears. *Science* 140 (1963), 1208–1211. **[2]** J. Bradley et al. *Nature* 301 (1983), 473–477. **[3]** H. Leroux et al. *GCA* 170 (2015), 247–265. **[4]** C. Alexander et al. *Geochem.* 77.2 (2017), 227–256. **[5]** H. Leroux. *LPSC XLIII, #1761* (2012). **[6]** S. Brenner. *Acta Metall.* 4.1 (1956), 62–74. **[7]** N. Abreu and A. Brearley. *MAPS* 46.2 (2011), 252–274. **[8]** E. Scott and A. Krot. *ApJ* 623.1 (2005), 571–578. **[9]** K. D. McKeegan et al. *Science* 332 (2011), 1528–1532. **[10]** D. Joswiak et al. *MAPS* 52.8 (2017), 1612–1648. **[11]** R. C. Ogliore et al. *MAPS* (2019). **[12]** A. N. Krot et al. *Science* 295.5557 (2002), 1051–1054. **[13]** A. N. Krot et al. *ApJ* 713.2 (2010), 1159. **[14]** L. Kööp et al. *LPI Contrib. 2083, #2706* (2018). **[15]** A. N. Krot et al. *GCA* 201 (2017), 185–223. **[16]** S. Kobayashi et al. *Geochem. J.* 37.6 (2003), 663–669. **[17]** R. C. Ogliore et al. *GCA* 166 (2015), 74–91. **[18]** L. Kööp et al. *GCA* 184 (2016), 151–172. **[19]** M. Gounelle et al. *ApJ* 698 (2009), L18–L22. **[20]** A. J. Fahey et al. *ApJ* 323 (1987), L91. **[21]** L. Kööp et al. *GCA* 189 (2016), 70–95. **[22]** A. N. Krot et al. *Chem. Erde-Geochem.* 64.3 (2004), 185–239. **[23]** F. J. Ciesla. *Science* 318.5850 (2007), 613–615.